Multidiszciplináris tudományok, 12. kötet. (2022) 3 sz. pp. 117-126 **https://doi.org/10.35925/j.multi.2022.3.11**

OPTIMIZATION OF NOTCHED TENSILE TEST SPECIMEN UNDER PLANE STRAIN CONDITION

Meknassi Raid Fekhreddine
PhD student, University of Miskolc, Institute of Mechanical Engineering and information, Department of Mechanical Technologies
3515 Miskolc, Miskolc-Egyetemváros, e-mail: metraid@uni-miskolc.hu

Béres Gábor
assistant professor, John von Neumann University, GAMF Faculty of Engineering and Computer Science, Kecskemét, Hungary, e-mail: beres.gabor@gamf.uni-neumann.hu

Lukács Zsolt
associate professor, University of Miskolc, Institute of Materials Science and Engineering, Department of Mechanical Technologies
3515 Miskolc, Miskolc-Egyetemváros, e-mail: zsolt.lukacs@uni-miskolc.hu

Abstract

In the current paper, specimen notch geometries during plane strain tensile test for cold-rolled steel DC01 is studied and optimized using Response Surface Methodology (RSM) and the desirability approach. The notch angle (X°), notch width (d), and notch length (c) were the main geometry parameters considered in this study. The effects of these parameters on the strain state were expressed by self-defined metrics, namely the Plane Strain State Index (PSSI) and the Homogeneity Index (HI) as well as those were analyzed by ANOVA analysis. The quadratic mathematical models obtained by the RSM presenting the evolution of the PSSI and the HI depending on (X°, d, and c) are presented. Optimization of the geometry parameters to achieve the optimal PSSI and better HI was carried out by a desirability function.

Keywords: *plane strain tension, RSM, sample notch, ANOVA analysis*

1. Introduction

The new generations of steels exhibit high strength and formability properties. These properties qualify these steel grades as a good choice for many applications in various engineering fields, especially the automotive industry. However, sheet metal forming processes for these types of steel are more complex than other steels due to high tensile strength, and high work hardening rate (Meknassi et al., 2021). For those reasons, many new technologies have been developed and are conducted to use complex tools and multi-stage forming processes in the actual industry.

Regarding that, much literature studied the effect of the multi-stage forming processes on the Forming Limit Diagrams (FLD) because it is considered the most used graphical tool for predicting the formability and safety limits of materials in sheet metal forming processes. (Lee et al., 1993) investigated the effect of discontinuous strain path on the FLD in sheet metal material. They observed that with strain histories where one of the principal strain increments is negative, the subsequent limit strains obtained from both theory and experiment are higher or lower than the ones obtained under the linear strain path.

(Gutiérrez et al., 2010) studied the effect of strain paths on the formability evaluation of TRIP steels. They found that uncertainty is created when complex or discontinuous strain paths are involved.

Recently, much research has been done to overcome this issue. One of these suggested methods is determining the FLD after applying two different load paths similar to the actual forming process industry by using a pre-strained specimen. In our work, we chose to deal with the plane strain state as pre-strain using tensile test followed by further tests. In order to do so, a pure plane strain specimen must be optimized.

In the current work, finite element simulations were used to study and measure the different strain behavior during the test. A model based on Response Surface Methodology (RSM) was used to establish the relationships between the three notch parameters: notch angle (X°), notch width (d), notch length (c), and the plane strain distribution, which is characterized by self-defined Plane Strain State Index (PSSI) and Homogeneity Index (HI) during the plane strain tensile test of DC01 cold rolled steel. Results were analyzed and optimized by the desirability approach as well.

2. Material and method

2.1. Material and sample geometry

In the present work we considered a nominal 1 mm thick, cold rolled steel (DC01). Mechanical properties parallel, perpendicular and 45°to the rolling direction are given in Tables 1. The plane strain tensile tests were performed by a geometry shown in Figure 1 (Wagoner et al., 1980). It was considered as the basic shape, on which subsequent improvements are proposed in this paper.

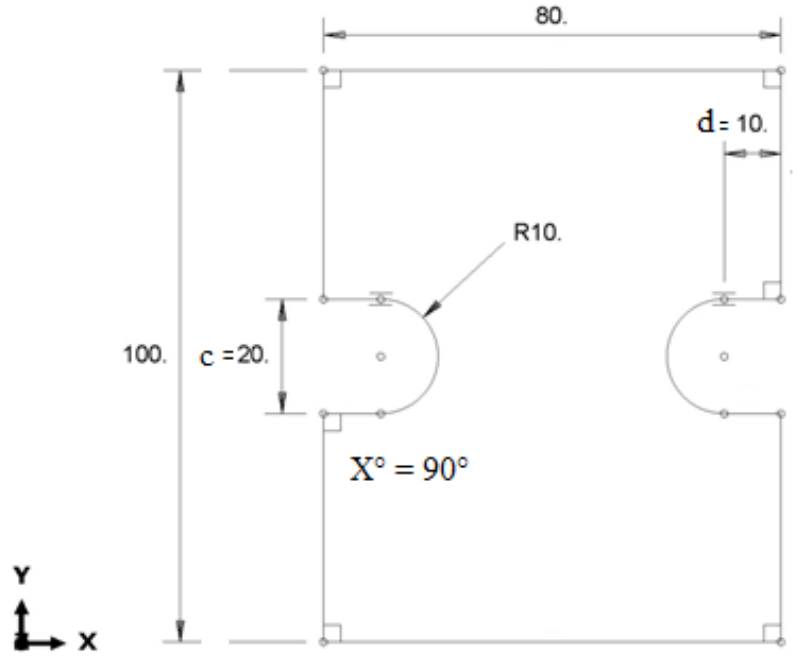

Figure 1. *Sample geometry, used in the plane strain tensile test simulation (units in mm)*

Table 1. *Data for the yield and strength parameters of DC01 material*

Orientation angle	A_{80} (%)	A_{80_ave} (%)	r	$\bar{r}$	Δr	$Rp_{0,2}$ (N/mm^2)	$Rp_{0,2\_ave}$ (N/mm^2)	R_m (N/mm^2)	R_{m_ave} (N/mm^2)
0°	40,0	38,0	2,35	1,99	0,88	199	201	306	309
45°	36,0		1,55			206		322	
90°	39,0		2,52			198		298	

Where: A80 is the total engineering strain, A80_ave is the average total engineering strain, r is the r-value, $\bar{r} = \frac{(r0+r90+2.r45)}{4}$ is the normal anisotropy, $\Delta r = \frac{(r0+r90)}{2-r45}$ is the planar anisotropy, $Rp_{0,2}$ is the yield strength, $Rp_{0,2\_ave}$ is the average yield strength, Rm is the tensile strength and R_{m_avr} is the average tensile strength.

2.2. Testing methods

To study the effect of various notch geometries (*X°, d, C*) on the strain field distributions, the *L27* (3^{13}) Taguchi standard orthogonal array is adopted as the testing method.

The factors and their levels in the present investigation and the orthogonal array *L27* of Taguchi method are presented in Table 2. The values chosen are as follows: notch angle (90, 95, and 100 degree), notch width (2.5, 5, and 10 mm), and notch length (15, 20, and 25 mm).

Table 2. *Factors and levels array*

Control parameters	Unit	Symbol	Levels		
			Level 1	Level 2	Level 3
Notch angle	degree	*X°*	90	95	100
Notch length	mm	*c*	15	20	25
Notch width	mm	*d*	2.5	5	10

For comparison of the different specimen geometries responses on the strain distribution, we used the following equations:

- Plane strain state index (*PSSI*): the closer the average minor strain ($\varepsilon_{\varepsilon 2}$) to zero, the better it is

$$PSSI = A_{\varepsilon 2} = \frac{\sum_{i=1}^{n} \varepsilon_2}{n} \quad (n = 1 \dots 9). \tag{1}$$

- Homogeneity index (*HI*) (equivalent with standard deviation): the smaller the *HI*, the better is the result, i.e. the strain distribution is more homogenous

$$HI = \sqrt{\frac{\sum_{i=1}^{n}(\varepsilon_1^n - A_{\varepsilon 1})^2}{n}} \quad (n = 1 \dots 9). \tag{2}$$

2.3. Finite element modelling

The code used for simulation was Abaqus 2021, with Hill (1948) yield criterion developed by Hill (1948) by defining six factors of plastic potentials R11, R22, R33, R12, R13, R23. Table 3. shows the analytical results obtained by the r-vaules that we used as input parameter in our work.

Table 3. *Analytical calculation results for Hill 48 plastic potential factors*

	R11	*R22*	*R33*	*R12*	*R13*	*R23*
DC01	1.00	1.01	1.31	1.12	1.00	1.00

In order to calculate the plastic stress–strain behavior of the investigated materials, the Swift non-linear isotropic hardening model, shown in equation (3), was used with the related data showed in Table 4. The parameters of the Swift equation were obtained by experimental tensile tests

$$\bar{\sigma} = K\,(\varphi_0 + \bar{\varphi})^n \tag{3}$$

Table 4. *Swift equation data*

Material	**Swift equation**		
	K [MPa]	***φ_0 [-]***	***N [-]***
DC01	578	0.02	0.22

During the simulations, all specimens have a 30 mm griping area length on both sides and 0.8 mm mesh size of a three-dimensional eight-node brick element with six integration points is used. The boundary and loading conditions are applied in a manner that is as similar to the real tensile test experiment as possible. The lower grip of the specimen was kept fixed in all directions but free in the direction of the applied load. The sliding between grips and specimen is neglected. The maximum major and minor strain values extracted in the strain hardening region before the local cross-sectional area becomes significantly smaller than the average (before 10% form the necking point). The data were gathered from nine different points in the middle area of all samples, as depicted in Figure 2.

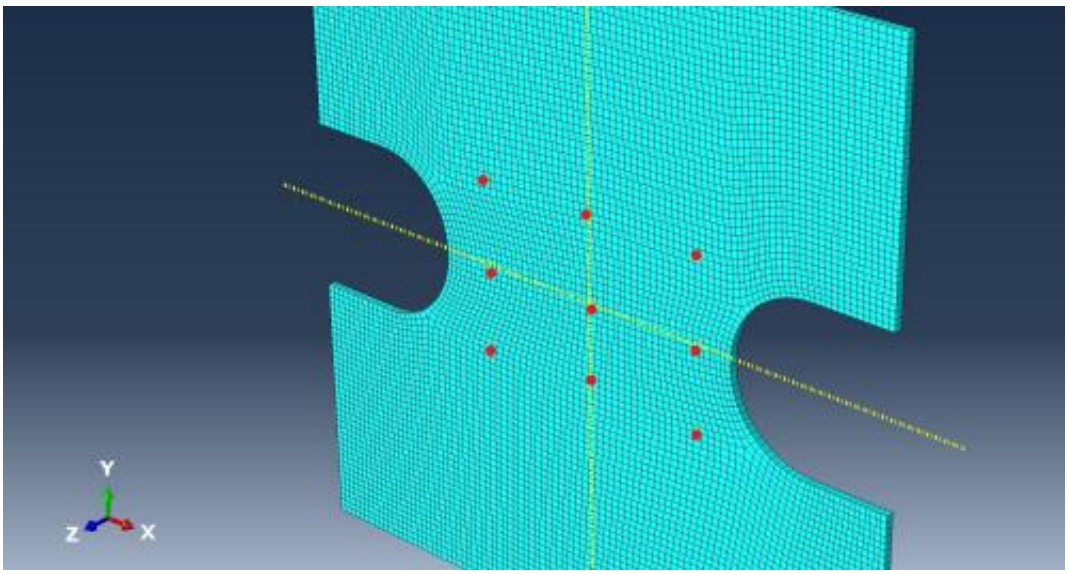

Figure 2. *Mesh and data points of the standard geometry*

3. Response surface methodology

The Analysis Of Variance (ANOVA) is a standard statistical technique commonly used to determine the significance of the independent variables on the output responses. It does not analyze the data directly but determines each factor's percentage of the contribution in determining the data's variability (variance). In the current study, the relationship between geometry conditions and strain distribution can be expressed as follows:

$$Y = \varphi(X°, c, d) \tag{4}$$

where φ is the response function and *Y* is the desired strain aspect. In the present work, the RSM-based second-order mathematical model is given by the following equation:

$$Y = \alpha 0 + \sum_{i=1}^{K} \beta i \, Xi + \sum_{i\,j}^{K} \beta ij \, Xi \, Xj + \sum_{i=1}^{K} \beta ii \, Xi^2 \tag{5}$$

where α_0 is the free term of the regression equation and the coefficients $\beta_1, \beta_2, \ldots, \beta_k$ and $\beta_{11}, \beta_{22}, \ldots, \beta_{kk}$ are the linear and the quadratic terms, respectively, while $\beta_{12}, \beta_{13}, \ldots, \beta_{k-1}$ are the interacting terms (Benardos et al., 2019; Bouzid et al., 2014).

4. Results and discussion

4.1. Analyze of variance

Table 5 shows all the response values of the examined factors. The objective is to analyze the influence of various combinations of the geometry parameters (*X°*, *d*, *c*) with complete factorial design on the total variance of the obtained results (*HI, PSSI*).

Tables 6 and 7 illustrate the ANOVA results for plane strain state index (PSSI) and homogeneity index (HI), respectively, for a 95% confidence level. In these tables, the values of Degrees of Freedom (DF), the sum of squared deviations (SS), mean square (MS), and the percentage of contribution (cont %) of each model term are listed. The primary purpose is to analyze the influence of the notch geometries (X°, d, C) on the total variance of the results. The sequential P-value is a statistical index used in the analysis of variance. In our models, we consider it less than 0.05, indicating that the models are adequate and that the terms significantly affect the desirable responses. We indicated the interactions between the the geometry parameters with A^2, B^2, C^2, AB, BC and AC, where A= X° , B= d,C= c.

Table 6 shows the ANOVA results for PSSI. It can be apparently seen that X° is the most crucial factor affecting PSSI. Its contribution is 57,91%. The second important term affecting PSSI is d with 16,50% of the contribution, followed by the product ($X^{\circ 2}$) and c with a contribution of 10,80%, and 6,62%, respectively. It can be assumed that the other terms are not significant.

From the analysis of Table 7, we can see that X° and c have a significant effect on HI. X° is the most significant factor with 34,84%. The next largest factor influencing HI is c, followed by d. Their contributions are 31.79% and 16,21% of the model. The other interactions are not essential and vary between 3,10% and 0,45%.

Table 5. *Orthogonal array for responses*

X°	*d (mm)*	*c (mm)*	*PSSI max*	*HI max*
	2.5	15	-0,1203	0,4168
	2.5	20	-0,0974	0,3175
	2.5	25	-0,0959	0,2898
	5	15	-0,0914	0,3811
	5	20	-0,0847	0,2304
	5	25	-0,0838	0,2057
	10	15	-0,0929	0,3350
	10	20	-0,0719	0,2168
90	10	25	-0,0435	0,1602
	2.5	15	-0,1329	0,7350
	2.5	20	-0,1018	0,3715
	2.5	25	-0,0996	0,2930
	5	15	-0,1133	0,4453
95	5	20	-0,1018	0,3715
	5	25	-0,0999	0,2630
	10	15	-0,0936	0,3570
	10	20	-0,0899	0,2476
	10	25	-0,0633	0,1914

100	2.5	15	-0,2435	0,9350
	2.5	20	-0,2235	0,7239
	2.5	25	-0,1986	0,4930
	5	15	-0,2345	0,7435
	5	20	-0,2105	0,4684
	5	25	-0,1850	0,3326
	10	15	-0,1532	0,5138
	10	20	-0,1403	0,5021
	10	25	-0,0995	0,2923

Table 6. *ANOVA results for PSSI*

Source	SS	DF	MS	F-Value	P-Value	Cont %	Remarks
Model	0.0760	9	0.0084	49.70	< 0.0001		significant
X°	0.0419	1	0.0419	246.77	< 0.0001	57,91%	significant
d	0.0120	1	0.0120	70.78	< 0.0001	16,50%	significant
c	0.0054	1	0.0054	31.51	< 0.0001	6,62%	significant
AB	0.0029	1	0.0029	17.03	0.0007	3,67%	significant
AC	0.0004	1	0.0004	2.18	0.1584	0,47%	Not significant
BC	0.0001	1	0.0001	0.8122	0.3800	0,17%	Not significant
A^2	0.0085	1	0.0085	50.14	< 0.0001	10,80%	significant
B^2	0.0002	1	0.0002	0.9117	0.3531	0,20%	Not significant
C^2	1.437E-08	1	1.437E-08	0.0001	0.9928	0,00%	Not significant
Residual	0.0029	17	0.0002			3,66%	
Total	0.0789	26				100,00%	

Table 7. *ANOVA results for HI*

Source	SS	DF	MS	F-Value	P-Value	Cont %	Remarks
Model	0.9040	9	0.1004	31.69	< 0.0001		significant
X°	0.3067	1	0.3067	96.79	< 0.0001	34,84%	significant
d	0.1719	1	0.1719	54.24	< 0.0001	16,21%	significant
c	0.2812	1	0.2812	88.71	< 0.0001	31,79%	significant
AB	0.0202	1	0.0202	6.38	0.0218	2,11%	significant
AC	0.0297	1	0.0297	9.38	0.0070	3,10%	significant
BC	0.0159	1	0.0159	5.02	0.0387	1,66%	significant
A^2	0.0188	1	0.0188	5.93	0.0262	1,96%	significant

B^2	0.0214	1	0.0214	6.76	0.0187	2,24%	significant
C^2	0.0043	1	0.0043	1.37	0.2580	0,45%	Not significant
Residual	0.0539	17	0.0032			5,62%	
Total	0.9579	26				100,00%	

4.2. Modelling by response surface methodology

The relationship between the factors and the output parameters was modelled by quadratic regression. The regression equations obtained are given below by Eqs. (6), and (7) with coefficients of determination R^2 of 96,34, and 94.38%, respectively. These regression models help predict the response of the parameters with respect to the input control parameters

$$PSSI\ max = -11{,}95 + 0{,}2671\ X° - 0{,}0791\ d - 0{,}0187\ c + 0{,}000814\ X° \,.\, d + 0{,}000222\ X° \,.\, C + 0{,}000177\ d \times C - 0{,}001507\ X°^2 + 0{,}000414\ d^2 - 0{,}000002\ C^2 \quad (6)$$

$$HI\ max = 14{,}45 - 0{,}346\ X° + 0{,}0792\ d + 0{,}1089\ C - 0{,}002150\ X° \,.\, d - 0{,}001991\ X° \,.\, C + 0{,}001908\ d \,.\, C + 0{,}002238\ X°^2 + 0{,}00487\ d^2 + 0{,}001076\ C^2 \quad (7)$$

The previous models can predict plane strain state index (PSSI) and homogeneity index (HI) in the range of selected sample geometries. Figures 3 and 4 illustrate the differences between the measured and predicted responses of HI and PSSI. These figures indicate that the quadratic models can represent the system under the given studied domain.

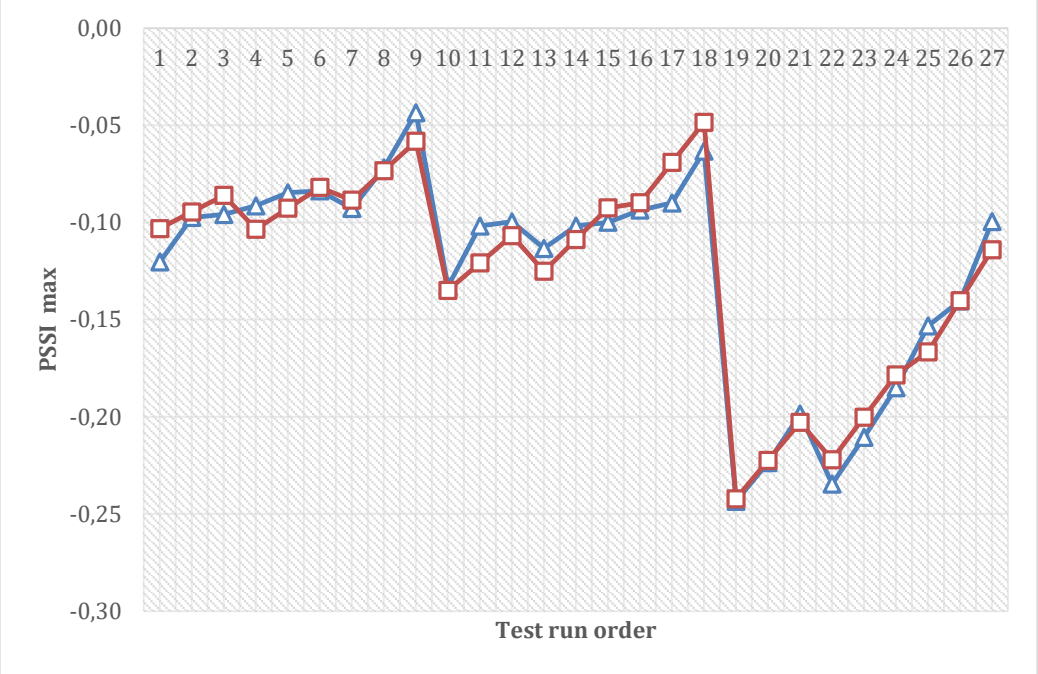

Figure 3. *Comparison of the measured (red color) and predicted (blue color)values for PSSI*

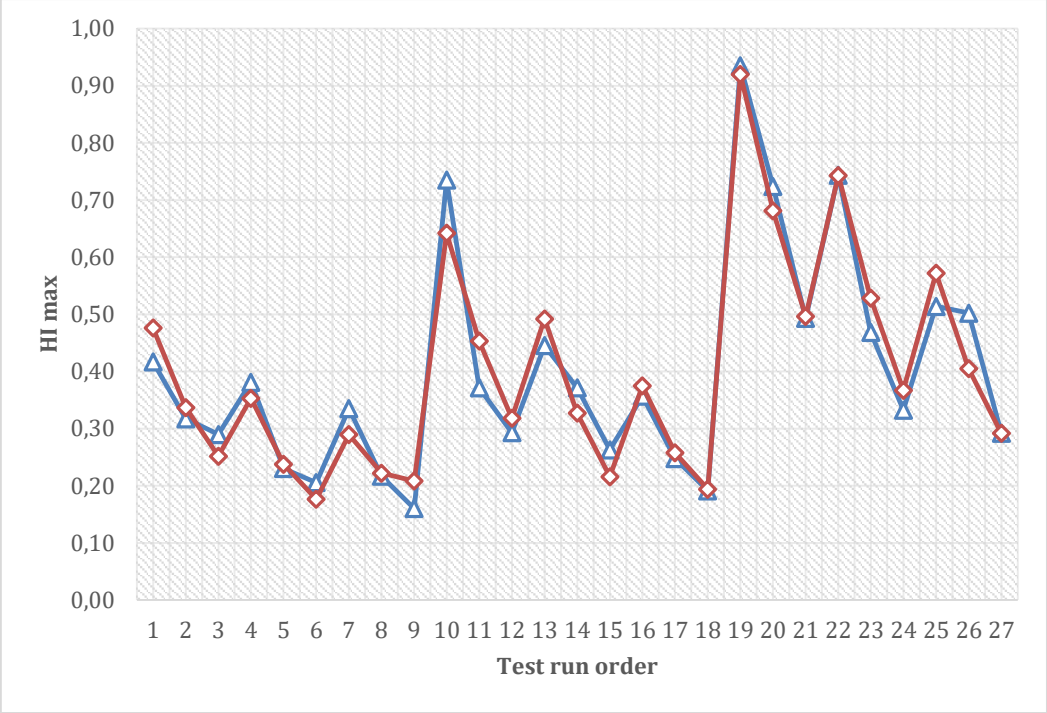

Figure 4. *Comparison of the measured (red color) and predicted (blue color) values for HI*

4.3. Optimization of responses using desirability function approach

The desirability function approach is one of the industry's most widely used methods for optimizing multiple response processes (Derringer et al., 1980).

Here, three optimization approaches are considered. The objective is to get the minimum of the plane strain state index (PSSI) and the homogeneity index (HI) simultaneously. The factor ranges defined for our optimization are summarized in Table 8.

Table 8. *Constraint for optimization of geometry conditions*

Name	Goal	Lower Limit	Upper Limit	Lower Weight	Upper Weight	Importance
X°	is in range	90	100	1	1	3
d (mm)	is in range	2.5	10	1	1	3
c (mm)	is in range	15	25	1	1	3
PSSI max	maximize	-0.243453	-0.0434691	1	1	5
HI max	minimize	0.160246	0.934983	1	1	5

Table 9 shows the results for the three optimization approaches. The optimal values are as follows: $X° = 93.14$, $d = 9.97$ mm, and $c = 25$ mm.

Table 9. *Optimization results*

Optimization	*X°*	*d (mm)*	*c (mm)*	*PSSI*	*HI*	Desirability
HI optimal	93.24	9.99	24.98	- 0.04	0.18	1
PSSI optimal	92.38	7.74	24.71	- 0.06	0.16	1
Combined	93.14	9.97	25	- 0.04	0.17	0.983

5. Summary

This study presents the numerical investigation of the strain state of a plane strain specimen supplemented by variance analysis. Three parameters were examined, namely the notch angle (X), the notch width (d) and the notch length (c). The ANOVA results showed that X° is the most important parameter influencing PSSI with a contribution of 57,91%, followed by d (16,50%). Furthermore, X° was identified as the most significant parameter the influences the HI (34,84%) followed by c (31.79 %). A comparing measured and predicted values present good agreements with the models found by response surface methodology. The results of the desirability function approach showed that the optimal parameters for maximal PSSI and minimal HI were found as (X° = 93.14, d = 9.97 mm, and c = 25 mm).

References

[1] Meknassi, R. F., Miklós, T. (2021). Third generation of advanced high strength sheet steels for the automotive sector: A literature review. *Multidiszciplináris Tudományok*, 11(4), 241-247. **https://doi.org/10.35925/j.multi.2021.4.28**

[2] Lee, T. C., Tsui, C. C., & Ho, K. W. (1993). *The effect of discontinuous strain path on the FLD in sheet metal material*. In Advances in Engineering Plasticity and its Applications (pp. 1105-1110). Elsevier. **https://doi.org/10.1016/B978-0-444-89991-0.50151-7**

[3] Gutiérrez, D., Lara, A., Casellas, D., & Prado, J. M. (2010). *Effect of strain paths on formability evaluation of TRIP steels*. In Advanced Materials Research (Vol. 89, pp. 214-219). Trans Tech Publications Ltd. **https://doi.org/10.4028/www.scientific.net/AMR.89-91.214**

[4] Wagoner, R. H. (1980). Measurement and analysis of plane-strain work hardening. *Metallurgical and Materials Transactions* A 11.1, 165-175. **https://doi.org/10.1007/BF02700453**

[5] Benardos, P. G., Vosniakos, G.-C. (2003). Predicting surface roughness in machining: a review. *International Journal of Machine Tools & Manufacture*, 43(8), 833-844. **https://doi.org/10.1016/S0890-6955(03)00059-2**

[6] Bouzid, L., Boutabba, S., Yallese, M. A., Belhadi, S., & Girardin, F. (2014). Simultaneous optimization of surface roughness and material removal rate for turning of X20Cr13 stainless steel. *The International Journal of Advanced Manufacturing Technology*, 74(5), 879-891. **https://doi.org/10.1007/s00170-014-6043-9**

[7] Derringer, G., Suich, R. (1980). Simultaneous Optimization of Several Response Variables. *Journal of Quality Technology*, 12, 214-219. **https://doi.org/10.1080/00224065.1980.11980968**